$$\frac{A(s,\theta)}{A_e(s)} = \int_z \int_r \rho(r,z) 2\pi r \cos(2\pi sz \cos\theta) J_0(2\pi sr \sin\theta)\, dr\, dz$$

$$= \int_z \int_r \rho(r,z) F(r,s,z,\theta)\, dr\, dz$$

$$= 4\Big[\int_{z=0}^{\nu a} \int_{r=0}^{\nu(a^2-z^2)^{1/2}} (\rho_{par} - \rho_0) F(r,s,z,\theta)\, dr\, dz + \int_{z=\nu a}^{\nu a+d} \int_{r=\nu(a^2-z^2)^{1/2}}^{\nu'(a'^2-z^2)^{1/2}} (\rho_{pol} - \rho_0) F(r,s,z,\theta)\, dr\, dz \Big]$$

ρ_{pal}, ρ_{pol}, and ρ_0 are respectively the electron density of the hydrocarbon core, the polar region, and the solvent. One gets

$$\frac{A(s,\theta)}{A_e(s)} = 4\Big[\int_{z=0}^{\nu a} \int_{r=0}^{\nu(a^2-z^2)^{1/2}} (\rho_{par} - \rho_0) F(r,s,z,\theta)\, dr\, dz + \int_{z=0}^{\nu a+d} \int_{r=0}^{\nu'(a'^2-z^2)^{1/2}} (\rho_{pol} - \rho_0) F(r,s,z,\theta)\, dr\, dz - \int_{z=0}^{\nu a} \int_{r=0}^{\nu(a^2-z^2)^{1/2}} (\rho_{pol} - \rho_0) F(r,s,z,\theta)\, dr\, dz \Big]$$

$$= 4\Big[\int_{z=0}^{\nu a} \int_{r=0}^{\nu(a^2-z^2)^{1/2}} (\rho_{par} - \rho_{pol}) F(r,s,z,\theta)\, dr\, dz + \int_{z=0}^{\nu a+d} \int_{r=0}^{\nu'(a'^2-z^2)} (\rho_{pol} - \rho_0) F(r,s,z,\theta)\, dr\, dz \Big]$$

with $\nu' = (\nu a + d)/(a + d)$ and $a' = (a + d)/\nu'$.

This is similar to the expression obtained for a sphere; one finds two terms in the expression of the scattered amplitude: the first one corresponds to an ellipsoid whose electron density is $(\rho_{par} - \rho_{pol})$, the second one to an ellipsoid with density $(\rho_{pol} - \rho_0)$.

Guinier and Fournet had given the expression of the form function of ellipsoids of revolution with axes $(R, R, \gamma R)$, electron density ρ and volume V

$$P(s) = (\rho - \rho_0)^2 V^2 \int_0^{\pi/2} \phi^2(2\pi Rsg(\theta)) \cos\theta\, d\theta \quad (A2)$$

where $\phi(u)$ is the form function of a sphere and $g(\theta) = (\cos^2\theta + \nu^2 \sin^2\theta)^{1/2}$.

Using this last equation, one obtains eq 3. Two cases must be considered: oblate or prolate ellipsoids.

(*a*) *Oblate Ellipsoids.* The revolution axis is the minor one. We use as parameter the smaller dimensiona of the hydrocarbon core, noted l_p. When the half-axes become l_{par}, l_{par}/ν and l_{par}/ν for the paraffinic core (with a volume $V_{par} = {}^4/_3\pi(l_{par}{}^3/\nu^2)$ and $l_{par} + d$, $l_{par}/\nu + d$ and $l_{par}/\nu + d$ for the whole particle (with a volume $V_{pol} = {}^4/_3\pi(l_{par}/\nu + d)^2(l_{par} + d)$).

In this case, $\nu < l$.

The form factor of these ellipsoids is then given by

$$P(s) = \int_0^{\pi/2} [V_{par}(\rho_{par} - \rho_{pol})\phi(g_1(\theta)2\pi l_{par}s) + V_{pol}(\rho_{pol} - \rho_0)\phi(g_2(\theta)2\pi(l_{par} + d)s)]^2 \cos\theta\, d\theta \quad (A3)$$

with $g_1(\theta) = (\cos^2\theta + \nu^2 \sin^2\theta)^{1/2}$, $g_2(\theta) = (\cos^2\theta + \nu'^2 \sin^2\theta)^{1/2}$, and $\nu' = \nu[(l_{par} + d)/(l_{par} + \nu d)]$.

(*b*) *Prolate Ellipsoids.* They are obtained by a rotation around the major axis. This time, their parameters are $(l_{par}, l_{par}, \nu l_{par})$ for the paraffinic part, $(l_{par} + d, l_{par} + d, \nu l_{par} + d)$ for the total particle with a volume $V_{pol} = {}^4/_3\pi(l_{par} + d)^2(\nu l_{par} + d)$, and $\nu > l$.

The expression of $P(s)$ (A3) can be used with $\nu' = (\nu l_{par} + d)/l_{par} + d$.

Registry No. Sodium OBS, 28675-11-8; 1-pentanol, 71-41-0.

Surface Density of States in the Many-Neighbor Approximation

S. G. Davison,*† D. A. Lavis,‡ and K. W. Sulston

Quantum Theory Group, Applied Mathematics Department, University of Waterloo, Waterloo, Ontario, Canada N2L 3G1 *(Received: July 29, 1985)*

The Green function for an infinite chain of atoms is calculated within the framework of the many-neighbor approximation. The Dyson equation is then used to derive the surface Green function of a semiinfinite chain, where the end atom is perturbed due to the presence of the surface. Results are presented and discussed for the surface density of states, and the conditions governing the existence of surface states are investigated.

1. Introduction

The initial calculations of the electronic properties of 1-dimensional solids in the many-neighbor approximation (MNA) were restricted to infinite systems.[1-3] The MNA is a molecular-orbital approach in which the nth nearest-neighbor (NN) interaction is written in the form $\beta_n = \beta\rho^{n-1}$, where β is the NN interaction energy and $|\rho| < 1$. The main effect on the bulk-band structure of including higher order interactions is to cause a broadening of the allowed bands with increasing ρ.

Since surface states (SS) of semiinfinite (or finite) crystals emerge from the band edges, it is clear that they too will be affected by the presence of MN interactions. However, the large number of surface boundary conditions, encountered as a result of the MN interactions, makes the study of such localized states via the molecular-orbital method an intractable problem. Fortunately, a Green function (GF) technique,[4] involving the use of the Dyson equation,[5] is available, which enables the numerous boundary conditions to be accommodated with comparative ease.

In the present paper, the GF G_0 for an infinite crystal is calculated in section 2. G_0 is then used in the Dyson equation to obtain the surface GF G_s for a semiinfinite crystal with a surface perturbation (section 3). The existence conditions for the SS are also given in section 3, and the numerical results for the surface density of states (SDOS) are presented and discussed in section 4. Concluding remarks are made in section 5.

2. Infinite Crystal

For an infinite, 1-dimensional crystal, in the MNA, the energy spectrum is given by[1]

† Department of Physics and the Guelph-Waterloo Program for Graduate Work in Physics.

‡ On leave from the Department of Mathematics, King's College (KQC), Strand, London WC2R 2LS, England.

(1) Davison, S. G.; Taylor, N. F. *Chem. Phys. Lett.* **1969**, *3*, 424.
(2) Davison, S. G. *Int. J. Quantum Chem.* **1972**, *6*, 387.
(3) Davison, S. G.; Foo, E. N. *Int. J. Quantum Chem.* **1976**, *10*, 867.
(4) Kalkstein, D.; Soven, P. *Surf. Sci.* **1971**, *26*, 85.
(5) Economou, E. N. "Green's Functions in Quantum Physics", 2nd ed.; Springer-Verlag: West Berlin, 1983; Solid State Sci. Ser., Vol. 7.

0022-3654/86/2090-0652$01.50/0

$$X(k) = (\cos ka - \rho)(1 - 2\rho \cos ka + \rho^2)^{-1} \quad (1)$$

where $X(k) = [E(k) - \epsilon]/2\beta$ is the *reduced energy*, $E(k)$ being the energy eigenvalue with wavenumber k, ϵ the 1-electron energy at each atom, and a the lattice constant. The corresponding GF for a *cyclic* crystal of N atoms may be written as

$$G_0(n,m) = \frac{1}{2\beta N}\sum_k \frac{e^{i(n-m)ka}}{X(k) - (\cos ka - \rho)(1 - 2\rho \cos ka + \rho^2)^{-1}} \quad (2)$$

In the limit, as $N \to \infty$, the sum in (2) can be replaced by a contour integral[5] around the unit circle in the complex plane of the variable $t = e^{ika}$, i.e., (2) becomes

$$G_0(n,m) = \frac{\eta}{i\pi}\oint \frac{t^{|n-m|}(t - \rho)(\rho t - 1)}{t(t - t_1)(t - t_2)}\,dt \quad (3)$$

where

$$\eta = [2\beta(2X\rho + 1)]^{-1} \quad (4)$$

$$t_{1,2} = \alpha \pm (\alpha - 1)^{1/2}(\alpha + 1)^{1/2} \quad (5)$$

$$\alpha = (2X\rho + 1)^{-1}(X\rho^2 + \rho + X) \quad (6)$$

Since (5) shows that

$$t_1 t_2 = 1 \quad (7)$$

the poles at t_1 and t_2 are *complex* inverse points with respect to the unit circle. When

$$(1 + \rho)^{-1} \leq X \leq (1 - \rho)^{-1} \quad (8)$$

$t_{1,2}$ lie *on* the unit circle, and (8) defines the band of extended states of an infinite crystal,[1] which corresponds to a branch cut of $G_0(n,m)$ in the complex X plane. A small positive imaginary part is included in X, so that $G_0(n,m)$ is defined uniquely for all X.

The contour integral (3) can then be evaluated from the residues at the poles $t = 0$ and $t = t_2$ of the integrand, which lie within the unit circle, to give

$$G_0(n,m) = 2\eta\rho\delta_{n,m} + \zeta t_2^{|n-m|} \quad (9)$$

where

$$\zeta = -i\eta[(1 - \rho)^{-1} - X]^{-1/2}[(1 + \rho)^{-1} + X]^{-1/2} \quad (10)$$

Because the atomic chain is infinite and homogeneous, the GF is translationally invariant, and can be written as

$$G_0(n,m) = g_0(n - m) \quad (11)$$

The GF is real, when X is real, except within the band of extended states given by (8), where the DOS expression is[5]

$$D_0(X,\rho) = -\pi^{-1}\,\mathrm{Im}\; g_0(0) \quad (12)$$

i.e.,

$$D_0(X,\rho) = \pi^{-1}\eta[(1 - \rho)^{-1} - X]^{-1/2}[(1 + \rho)^{-1} + X]^{-1/2} \quad (13)$$

As in the NN situation, the DOS exhibits the same square root Van Hove singularity at the band edges. This can be understood in terms of the real-space rescaling analysis of Lavis et al.,[6] since the fixed point controlling the band edges lies in the subspace $\rho = 0$, which is the same as that for the NN model.

3. Surface Green Function

A semiinfinite, 1-dimensional crystal can be formed from an infinite one by passing a cleavage line between the atoms on sites $m = 0$ and -1. In second-quantized form, the scattering potential in the MNA is

$$V_c = -\sum_{n=1}^{\infty}\beta_n\sum_{m=0}^{n-1}(|m - n\rangle\langle m| + |m\rangle\langle m - n|) \quad (14)$$

where

$$\beta_n = \beta\rho^{n-1}, \quad |\rho| < 1 \quad (15)$$

is the resonance integral between nth NN atoms.

The creation of a surface at the end of a semiinfinite crystal perturbs the electronic environment in the region. The perturbation can be taken into account by changing the site energy from ϵ to ϵ_0 for the surface atom at $n = 0$, and altering the values of the MN interactions with the surface atom from β_n to γ_n, where, by analogy with (15),

$$\gamma_n = \gamma\sigma^{n-1}, \quad |\sigma| < 1 \quad (16)$$

In this case, the surface perturbation potential can be written as

$$V_p = |o\rangle(\epsilon_0 - \epsilon)\langle o| + \sum_{n=1}^{\infty}(\gamma_n - \beta_n)(|o\rangle\langle n| + |n\rangle\langle o|) \quad (17)$$

Combining (14) and (17) leads to the total surface perturbation potential, which can be expressed as

$$V_s = V_c + V_p = (\epsilon_0 - \epsilon)|o\rangle\langle o| - \sum_{m=1}^{\infty}\sum_{n=1}^{\infty}\beta_{n+m}(|-n\rangle\langle m| + |m\rangle\langle -n|) - \sum_{n=1}^{\infty}\beta_n(|-n\rangle\langle o| + |o\rangle\langle -n|) + \sum_{n=1}^{\infty}(\gamma_n - \beta_n)(|o\rangle\langle n| + |n\rangle\langle o|) \quad (18)$$

The Greenian operator for the perturbed semiinfinite crystal is given by Dyson's equation[5] in the form

$$G_s = G_0 + G_0 V_s G_s \quad (19)$$

Substituting (18) in (19), noting that $G_s(m,n) = 0$, if m and n refer to sites on *opposite* sides of the cleavage line,[4] and introducing the matrix notation

$$g_s(n) = \langle n|G_s|o\rangle \quad (20)$$

eventually leads to the surface GF equation for the surface atom at $n = 0$, viz.,

$$Sg_s(0) + \zeta T_1(\rho)\Sigma_1 - g_0(0)(\Sigma_2 + 1) = 0 \quad (21)$$

where

$$T_j(\theta) = (t_j - \theta)^{-1}; \quad j = 1, 2; \quad \theta = \rho, \sigma \quad (22)$$

$$S = 1 - (\epsilon_0 - \epsilon)g_0(0) + \zeta[2\beta T_1(\rho) - \gamma T_1(\sigma)] \quad (23)$$

$$\Sigma_1 = \sum_{m=1}^{\infty}\beta\rho^m g_s(m)$$

$$\Sigma_2 = \sum_{m=1}^{\infty}(\gamma\sigma^{m-1} - \beta\rho^{m-1})g_s(m) \quad (24)$$

After some lengthy algebra, (18) and (19) give the expression

$$g_s(m) = t_2^m\zeta\{1 + (\epsilon_0 - \epsilon)g_s(0) - T_1(\rho)[\Sigma_1 + \beta g_s(0)] + [\gamma T_2(\sigma) - \beta T_2(\rho)]g_s(0) + \Sigma_2\} + [\gamma\lambda(\sigma)\sigma^{m-1} + \beta\lambda(\rho)\rho^{m-1}]g_s(0) \quad (25)$$

where

$$\lambda(\theta) = \left[\frac{\theta\zeta(t_2 - t_1)}{1 + \theta^2 - 2\theta\alpha} + 2\eta\rho\right]; \quad \theta = \rho, \sigma \quad (26)$$

which by (5), (6), and (11) becomes

$$\lambda(\theta) = 2\eta\left[\frac{(\rho - \theta)(1 - \rho\theta)}{1 + \theta^2 - 2\theta\alpha}\right]; \quad \theta = \rho, \sigma \quad (27)$$

Thus, (27) shows that $\lambda(\rho) = 0$ in (25).

(6) Lavis, D. A.; Davison, S. G.; Southern, B. W., to be published.

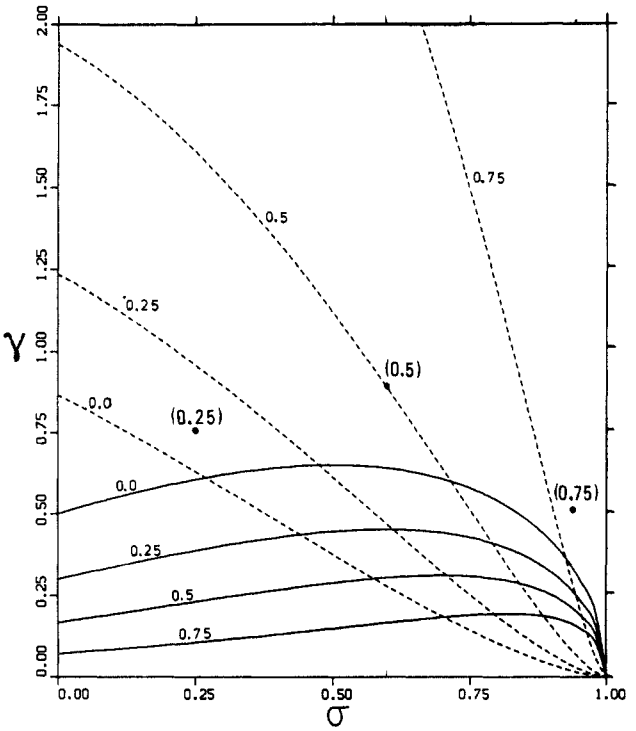

Figure 1. Surface state existence curves for $\epsilon_0 = -0.5$ and labeled with their values of ρ. Broken (solid) lines correspond to condition for surface state above (below) the band. Large dots with ρ values in parentheses correspond to curves plotted in Figures 2–4.

Multiplying (25) first by $\beta\rho^m$ and then by $(\gamma\sigma^{m-1} - \beta\rho^{m-1})$, and summing the results separately over the range $1 \leq m \leq \infty$, leads to two other linear equations in $g_s(0)$, Σ_1, and Σ_2, i.e.,

$$Ag_s(0) + P_1\Sigma_1 - P_2(\Sigma_2 + 1) = 0 \tag{28}$$

$$Bg_s(0) + Q_1\Sigma_1 + Q_2(\Sigma_2 + 1) = 1 \tag{29}$$

where

$$A = P_2C - \beta\gamma\rho\lambda(\sigma)(1 - \rho\sigma)^{-1}$$

$$B = Q_1T_1^{-1}(\rho)C - \gamma\lambda(\sigma)[\gamma(1 - \sigma^2)^{-1} - \beta(1 - \rho\sigma)^{-1}]$$

$$C = \beta T_1(\rho) - \gamma T_2(\sigma) + \beta T_2(\rho) - (\epsilon_0 - \epsilon) \tag{30}$$

$$P_1 = 1 + T_1(\rho)P_2, \quad P_2 = \zeta\rho\beta T_1(\rho)$$

$$Q_1 = \zeta T_1(\rho)[\gamma T_1(\sigma) - \beta T_1(\rho)], \quad Q_2 = 1 - Q_1T_1^{-1}(\rho)$$

Equations 21, 28, and 29 can now be solved by Cramer's rule to give the surface GF

$$g_s(0) = \Delta_1\Delta^{-1} = \Delta_1 \begin{vmatrix} S & & \Delta_1 & \\ A & & & \\ B & Q_1 & & Q_2 \end{vmatrix}^{-1} \tag{31}$$

where

$$\Delta_1 = \begin{vmatrix} \zeta T_1(\rho), & -g_0(0) \\ P_1, & -P_2 \end{vmatrix} \tag{32}$$

Proceeding further, the SS energies X_s are given by the zeros of Δ in (31). We shall, without loss of generality, fix the zero and scale of energy be setting $\epsilon = 0$ and $\beta = 0.5$, so the existence conditions then become

$$\gamma^2 > \mp\frac{1}{2}\left(\frac{1 \pm \rho}{1 \mp \rho}\right)\left[\epsilon_0 \mp \frac{1}{(1 \mp \rho)}\right]\left[\frac{(1 \mp \sigma)^2(1 - \sigma^2)}{(1 - \rho\sigma)^2}\right] \tag{33}$$

where the upper (lower) sign refers to a SS above (below) the band. When $\rho = \sigma = 0$, (33) reduces to the localized state condition of Lavis et al.[7]

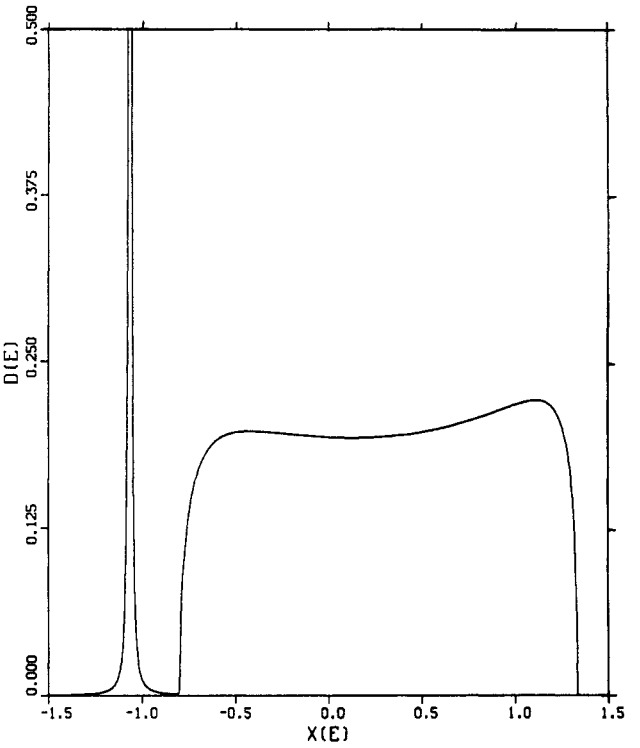

Figure 2. Surface density of states curve for $\rho = 0.25$, $\epsilon_0 = -0.5$, $\gamma = 0.75$, and $\sigma = 0.25$ showing surface state below the band.

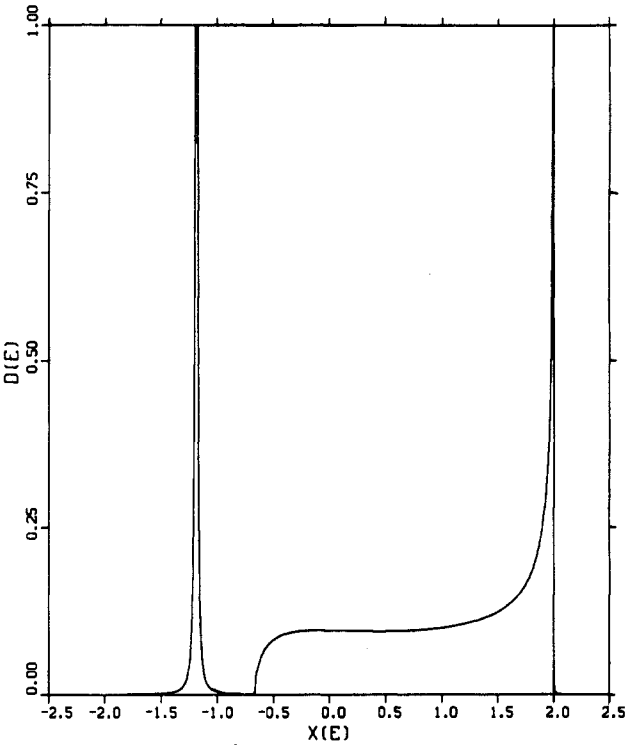

Figure 3. Surface density of states curve for $\rho = 0.5$, $\epsilon_0 = -0.5$, $\gamma = 0.885$, and $\sigma = 0.6$ showing surface state below the band and singularity at upper band edge.

4. Results and Discussion

The inequality, eq 33, gives a lower bound on γ for the existence of SS. The lower bound curves are drawn in Figure 1 for $\epsilon_0 = -0.5$, as functions of σ, and labeled with their values of ρ. The broken (solid) lines correspond to the condition for a SS to lie above (below) the band. Thus, for a particular value of ρ, the $\gamma\sigma$ plane is divided into various existence regions bounded by the

(7) Lavis, D. A.; Southern, B. W.; Davison, S. G. *J. Phys. C.* **1985**, *18*, 1387.

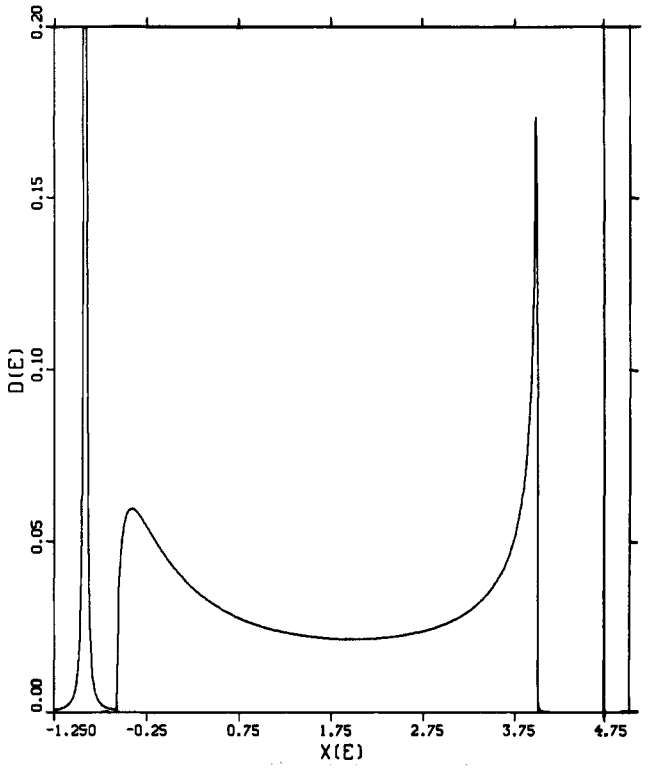

Figure 4. Surface density of states curve for $\rho = 0.75$, $\epsilon_0 = -0.5$, $\gamma = 0.5$, and $\sigma = 0.9$ showing surface states above and below the band.

curves corresponding to that value of ρ.

From (12) and (31), the SDOS can be computed numerically. The results obtained are shown in Figures 2–4 for the parametric values corresponding to the three large dots identified in Figure 1 by the ρ values shown in parentheses. Figure 2 depicts the SDOS curve for the first dot at $\rho = 0.25$, $\epsilon_0 = -0.5$, $\gamma = 0.75$, and $\sigma = 0.25$. The SS below the lower band edge is located by including a small imaginary part in the energy E in this range. The δ-function singularity then becomes a narrow Gaussian curve. The graph of Figure 3 shows the SDOS for the second dot at $\rho = 0.5$, $\epsilon_0 = -0.5$, $\gamma = 0.885$, and $\sigma = 0.6$. Here the SS below the lower band edge is accompanied by a singularity at the upper band edge. In the case of Figure 4, for the third dot at $\rho = 0.75$, $\epsilon_0 = -0.5$, $\gamma = 0.5$, and $\sigma = 0.9$, a SS occurs on both sides of the band. Comparing Figures 2–4, an increase in the bandwidth is observed, together with a shift to higher values of $X(E)$. Moreover, the emergence of the SS from the upper band edge distorts the band SDOS in this region.

5. Conclusion

The SDOS of a semiinfinite monoatomic chain of atoms has been studied, within the context of the MNA, by using the Dyson equation approach. A detailed analysis of the SS existence conditions was undertaken and related to the structure of the SDOS curves. As is apparent from the results and discussion presented in the previous section, the inclusion of higher order interactions has a marked effect on the SDOS. Finally, it should be noted that, while the treatment described here has been concerned with 1-dimensional crystals, the findings are also valid for long-chain polyenes.

Acknowledgment. The work reported here has been supported by the Natural Sciences and Engineering Research Council (NSERC) of Canada. S.G.D also wishes to thank NSERC and the Royal Society of London for a grant awarded under the auspices of the Anglo-Canadian Scientific Exchange Scheme, which enabled him to visit the Department of Mathematics at Chelsea College, University of London, England. We are grateful to B. W. Southern for many useful conversations.

Dynamics of Micellar Solutions of Ionic Surfactants by Fluorescence Probing

Angelos Malliaris,† Jacques Lang,‡ and Raoul Zana*‡

NRC "Demokritos", Athens, Greece, and ICS (CRM-EAHP) and Grêco Microémulsion, 67000 Strasbourg, France *(Received: August 7, 1985)*

Photophysical evidence is presented indicating that in aqueous solutions of ionic surfactants, under appropriate conditions of the nature of the surfactant, surfactant concentration, and ionic strength, fast intermicellar exchange of micelle-solubilized pyrene or cetylpyridinium ion can occur on a time scale of 0.3–10 μs. Furthermore it is shown that this process is not the result of micellar collisions as it is known to be the case in water-in-oil microemulsions. On the basis of the results, it is proposed that the observed intermicellar migration is due to fragmentation of the micelles into submicellar aggregates or fragments. One of the fragments carrying the solubilizate subsequently associates with a micelle (coagulation). Successive fragmentation/coagulation reactions result in solubilizate migration. This mechanism permits us to explain all of our experimental results. The relationship between the results of the present investigation and of previous chemical relaxation studies is discussed.

Introduction

Time-resolved fluorescence quenching of micelle-solubilized fluorescent probes by appropriate quenchers has found wide applications during the past decade[1] in determining the dynamic behavior and characteristic parameters of aqueous micelles,[2,3] alcohol swollen micelles,[4,5] microemulsions,[5] etc. A typical fluorescent probe, systematically employed for such studies, is pyrene (P) because of its very low solubility in water and its exceptionally small fluorescence decay rate constant k_0.[6] On the other hand, the numerous quenchers available can be classified into two main categories according to the relationship between their residence time in a micelle and the unquenched fluorescence

†NRC "Demokritos".
‡ICS (CRM-EAHP) and Grêco Microémulsion.

(1) Singer, L. A. In "Solution Behavior of Surfactants", Mittal, K. L., Fendler, E., Eds.; Plenum Press: New York, 1982; Vol. I, p 73.
(2) Lianos, P.; Lang, J.; Zana, R. *J. Colloid Interface Sci.* **1983**, *91*, 276, and references therein.
(3) Malliaris, A.; Le Moigne, J.; Sturm, J.; Zana, R. *J. Phys. Chem.* **1985**, *89*, 2709.
(4) Lianos, P.; Lang, J.; Sturm, J.; Zana, R. *J. Phys. Chem.* **1984**, *88*, 819, and references therein.
(5) Lianos, P.; Zana, R. *J. Colloid Interface Sci.* **1984**, *101*, 587.
(6) Thomas, J. K. *Chem. Rev.* **1980**, *80*, 283.

0022-3654/86/2090-0655$01.50/0